J Electr Eng Technol.2015;10(1): 227-242
http://dx.doi.org/10.5370/JEET.2015.10.1.227

ISSN(Print) 1975-0102
ISSN(Online) 2093-7423

Imposed Weighting Factor Optimization Method for Torque Ripple Reduction of IM Fed by Indirect Matrix Converter with Predictive Control Algorithm

Muslem Uddin*, Saad Mekhilef†, Marco Rivera and Jose Rodriguez*****

Abstract – This paper proposes a weighting factor optimization method in predictive control algorithm for torque ripple reduction in an induction motor fed by an indirect matrix converter (IMC). In this paper, the torque ripple behavior is analyzed to validate the proposed weighting factor optimization method in the predictive control platform and shows the effectiveness of the system. Therefore, an optimization method is adopted here to calculate the optimum weighting factor corresponds to minimum torque ripple and is compared with the results of conventional weighting factor based predictive control algorithm. The predictive control algorithm selects the optimum switching state that minimizes a cost function based on optimized weighting factor to actuate the indirect matrix converter. The conventional and introduced weighting factor optimization method in predictive control algorithm are validated through simulations and experimental validation in DS1104 R&D controller platform and show the potential control, tracking of variables with their respective references and consequently reduces the torque ripple.

Keywords: AC-AC power conversion, Induction motor, Matrix converter, Predictive control, Weighting factor

1. Introduction

The prevalent control of torque than speed has made direct torque control (DTC) as an important control algorithm for induction motor with variable speed drives due to its fast transient responses. Hysteresis phenomena based DTC has some drawbacks, such as: firstly, variable switching frequency and dependency on the hysteresis band and induction motor speed and secondly, considerable torque ripples compared to field oriented control. These torque ripples in DTC can be minimized by reducing the sampling interval which causes high switching frequency and are responsible for high switching losses. As a result, recently some inquisitions are more focused with the DTC, utilizing space vector modulation [1] and predictive torque control (PTC) and intelligent control for torque ripple reduction of induction motor drives in [2]. In [3], a study has been carried out with the combination of predictive control algorithm and DTC control. The analyses put the predictive control is the most powerful control algorithm and simple to implement due to its characteristics features.

† Corresponding Author: Department of Electrical Engineering, University of Malaya, Kuala Lumpur, Malaysia. (saad@um.edu.my)
* Power Electronics and Renewable Energy Research Laboratory (PEARL), Department of Electrical Engineering, University of Malaya, Kuala Lumpur, Malaysia. (muslem_eee04@siswa.um.edu.my)
** Department of Industrial Technologies, Universidad de Talca, Curico, Chile. (marcoriv@utalca.cl)
*** Departamento de Electrónica, Universidad Técnica Federico Santa María. (UTFSM), Chile. (jrp@usm.cl)
Received: September 3, 2013; Accepted: August 31, 2014

AC-AC power conversion is very much important and extensively used in industries. The DC-link storage elements (capacitor or inductor) are convenient for decoupling of control process but energy storage components are usually large in size and responsible for reducing the life span of the converter. To overcome all these disadvantages, different topologies on AC-AC power converter have been investigated in literature and classified in three main groups, such as: 1) cycloconverter; 2) direct matrix converter (DMC) and 3) indirect matrix converter (IMC) [4]. The conversion of power (AC-AC) in cycloconverter are accomplished in absent of intermediate energy storage devices which reduces the size and increases life time of the converter but it has a great limitation with output frequency which consists of significant harmonic contents due to the switching commutations and these harmonic contents can't be reduced by load inductance. In the DMC, an array of (3×3) bidirectional switches directly connected to the load from grid without any intermediate DC-link storage devices but its control is highly complex and sophisticated. Therefore, to overcome all the limitations stated above, the indirect matrix converter topology has been investigated which offers similar performance to DMC, but the most important improvement of this topology is the simpler and less complex in the control compare to the DMC and allowing secure commutations of the system [5] without particular sensing devices as needed for DMC [6].

Furthermore, the investigation concern to torque control

of induction motor have been carried out in [7] considering back-to-back and matrix converters (MCs) with pulse width modulation (PWM) schemes maintaining the pure sinusoidal output current and unity power factor. Recently, some new research works on multilevel inverters in [8-11], an advanced cascade multilevel converter for reduced number of components [12], synchronous PWM for the Fly back converter [13] and symmetrical sampling digital PWM for power converters in [14] have been introduced in literature. Different applications in the active front end rectifier [15, 16], voltage source inverter [17] and matrix converter [18], three-level boost converter and an NPC inverter for high-power PMSG-based medium voltage wind energy conversion systems [19] with predictive control algorithm have been successfully investigated in recent years. Also, an online parameter estimation of PMSM using an extended Kalman-Filter has been proposed in [20]. The predictive control technique have been applied in the IMC for different investigations such as, current control [21], current control extended by reactive power minimization [22], implementation of virtual damping resistance to mitigate the resonance effect due to low damped input filter [18], torque-flux control with unity power factor in [23] and imposed sinusoidal load and source currents in [24]. A MPC method has been applied with decoupled of active and reactive power control for high power grid-connected four-level diode-clamped inverters in [25].

Diverse control variables, targets and constraints can be included in a single cost function with the finite control set model predictive control (FCS-MPC) and simultaneously be controlled with the basis of priority control factor is known as weighting factor. If the variables are in same feature then no need to set the weighting factor but when the target variables are in different nature (different order of magnitude and different unit) in a single cost function then weighting factor selection become as a great issue and deteriorates the performance of the system greatly.

In literature, it have been introduced several types of terms that can be included in a cost function and shows how these terms are related to different control design requirements for the system. Depending on the nature of the different terms involved in the formulation of the cost function, they can be classified in different groups, such as: cost function without weighting factor in which no need to set the weighting factor applied in [17, 26, 27] and [28]; cost function with weighting factor in the secondary term investigated in [29, 30]; cost function with equally important terms proposed in [23]. Till the date in literature no analytical or numerical methods or control design theories to adjust the weighting factor for equally important term and currently they are evaluated with the iterative evaluation method [31].

This method is extensively used to adjust the weighting factor. However, with this method the weighting factor can be adjusted and potential performances can be attained but this is quietly approximated. So, this weighting factor should be optimized to get optimized best performances of the system. In recent past, an optimization method of weighting factor calculation to ensure the optimized actuations to the three phase voltage source inverter (VSI) and IMC for controlling torque-flux of the induction motor have been introduced in [32, 33] and [34], respectively and better performance has been achieved comparative to conventional weighting factor adjustment followed by iterative evaluation method. Recently, a novel predictive two-level inverter fed induction motor control strategy with weighting factor look up table and divide control interval have been investigated in [35]. In [36], a ranking approach based multi-objective optimization has been proposed to replace the single cost function at the predictive horizon which allows the predictive control of torque and flux without weighting factors. To improve the speed control of IM, a continuous-time Poisson-Laguerre model based adaptive predictive controller has been applied successfully in [37] and different loss analysis at IM was investigated in [38].

This paper proposes an optimization method of weighting factor used in predictive control algorithm to reduce the torque ripple as well as flux control of the induction motor fed by an indirect matrix converter (IMC). The torque ripple behavior are analyzed in both the rated and low speed region of the induction motor and compared to conventional weighting factor based predictive control method.

This paper is organized in the following sequence: Section 2 is related to the mathematical modeling of the indirect matrix converter (IMC) topology and inductive load of the system. Section 3, present the proposed weighting factor optimization method to reduce the torque ripples in the predictive control platform. Section 4 states, verification results and discussion of the proposed method to reduce the torque ripple than the conventional weighting factor based MPC method. Section 5 depicts the experimental results. Finally, a fruitful conclusion is drawn in section 6.

2. Modeling of Indirect Matrix Converter Topology

The topology of IMC is shown in Fig. 1 consists of a rectifier part and an inverter part. Here, the DC-link voltage is obtained as a function of rectifier switches (S_r) and input voltages (V_i) of the converter,

$$V_{dc} = \begin{bmatrix} S_{1r} - S_{4r} & S_{3r} - S_{6r} & S_{5r} - S_{2r} \end{bmatrix} V_i \quad (1)$$

where S_{1r} to S_{6r} are the rectifier switching states and input voltage $V_i = \begin{bmatrix} V_i^a & V_i^b & V_i^c \end{bmatrix}^T$. The rectifier input current I_{ri} is defined as a function of the rectifier switches and DC-

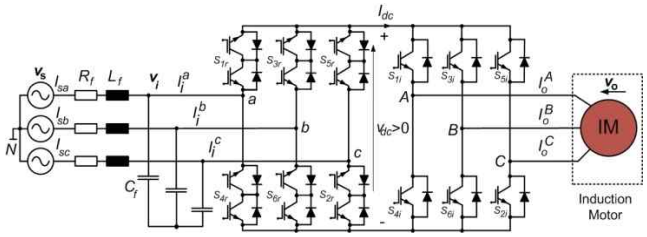

Fig. 1. Indirect matrix converter fed induction motor.

link current I_{dc} as,

$$I_{ri} = \begin{bmatrix} S_{1r} - S_{4r} \\ S_{3r} - S_{6r} \\ S_{5r} - S_{2r} \end{bmatrix} I_{dc} \tag{2}$$

In Eq. (2) the input currents are given as, $I_{ri} = \begin{bmatrix} I_i^a & I_i^b & I_i^c \end{bmatrix}^T$. On the other side, the modeling of the inverter part is as,

$$V_o = \begin{bmatrix} S_{1i} - S_{4i} \\ S_{3i} - S_{6i} \\ S_{5i} - S_{2i} \end{bmatrix} V_{dc} \tag{3}$$

$$I_{dc} = \begin{bmatrix} S_{1i} & S_{3i} & S_{5i} \end{bmatrix} I_o \tag{4}$$

Here, $V_o = \begin{bmatrix} V_o^A & V_o^B & V_o^C \end{bmatrix}^T$ is the output voltage and $I_o = \begin{bmatrix} I_o^A & I_o^B & I_o^C \end{bmatrix}^T$ corresponds to the output current.

In this IMC topology, not only rectifier model corresponds to nine valid possible switching states but also inverter is associated with eight valid possible switching states. But to satisfy the constraints of IMC the possible switching states are only 24.

2.1 Inductive load model

A two dimensional space vector (SV) can be represented from three phase quantities of the converter to obtain the system of the model. For example complex space vector described from the three phase quantities y_A, y_B and y_C are given as,

$$\mathrm{y} = \mathrm{y}_\alpha + jy_\beta \tag{5}$$

$$\text{where, } y_\alpha = \frac{1}{3}(2y_A - y_B - y_C), \; y_\beta = \frac{1}{\sqrt{3}}(y_B - y_C) \tag{6}$$

In Eq. (6), stationary reference frame ($\alpha\beta$ -reference frame) is considered for expected space vector (SV). The model of the induction motor referred to stator is obtained as described in [39]. Fixed coordinate rotor and stator voltage equations are presented as,

$$V_o = R_s I_o + L_s \dot{\psi}_s \tag{7}$$

$$V_r = R_r I_r + L_r \dot{\psi}_r - jp\omega\psi_s \tag{8}$$

where R_s, R_r, p and ω are the stator resistance, rotor resistance, number of pole pairs and rotor angular frequency, respectively. The stator flux and rotor flux are related with the following equations,

$$\psi_s = L_s I_o + L_m I_r, \;\; \psi_r = L_r I_r + L_m I_o \tag{9}$$

where, L_s, L_r are self-inductances and L_m is the mutual inductance of the induction motor. Finally, electrical torque is developed in the induction motor can be represented by stator current and flux terms,

$$T_e = \frac{3}{2} p(\psi_s \times I_o) \tag{10}$$

3. Proposed Predictive Control Algorithm with Weighting Factor Optimization Method

Predictive control algorithm uses the finite number of valid switching states of the power converter. The proposed scheme maintains the predictive values closed to their respective references at the end of the sampling instant and maintain the positive DC-link voltage between the rectifier and inverter stages. The proposed predictive control scheme and algorithm with weighting factor optimization are presented in Figs. 2 and Fig. 3, respectively. Predictive controller satisfies the following five steps:

Steps 1: Supply voltage V_s^k, input voltage V_i^k, stator current I_o^k and speed ω^k of the induction motor are measured in the k^{th} sampling instant.

Step 2: PI controller is used to set nominal torque T_{nom} from the error signal between the measured and reference speeds of the induction motor where reference speed ω_{ref} is known value. Here, PI controller gains are taken with the trial and error

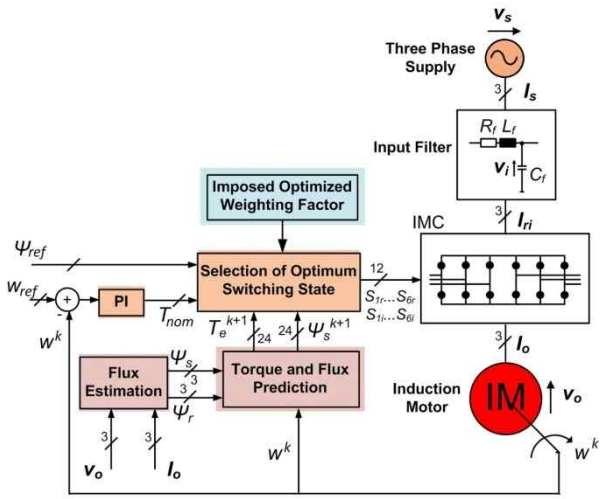

Fig. 2. Proposed control scheme with weighting factor optimization.

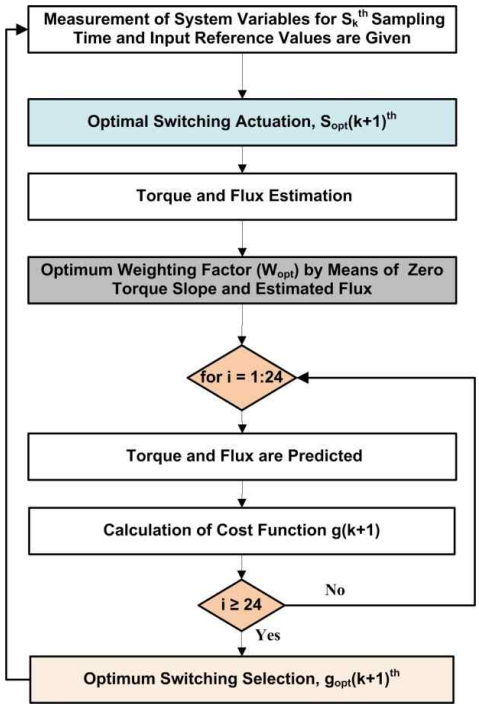

Fig. 3. Predictive torque and flux control flow diagram.

method for tuning the output. The final tuning values used in this investigation are*;* Kp =1 and Ki = 512.82.

Step 3: Stator reference flux ψ_{ref} is a given value and a flux estimator has been used to estimate the stator and rotor flux.

Step 4: For each valid switching states of indirect matrix converter, values of torque T_e^{k+1} and stator flux ψ_s^{k+1} are predicted utilizing the optimum weighting factor in the next sampling period (k+1).

Step 5: All the predictive values are compared with their respective references and determine the cost functions for all possible switching states based on conventional weighting factors and with imposed optimized weighting factor. The switching state corresponds to the minimum cost function is selected in the next sampling time period to actuate the converter.

3.1 Torque and flux prediction

The induction motor model has explained in Eqs. (7)-(10) are used with first order approximation for derivatives along with the first order nature of state equations,

$$y = \frac{y^{k+1} - y^k}{T_s} \tag{11}$$

where T_s is the sampling period; so, rotor and stator--flux can be estimated from (7)-(8) resulting in,

$$\psi_s^k = \psi_s^{k-1} + V_o^k T_s - R_s I_o^k T_s \tag{12}$$

$$\psi_r^k = I_o^k (L_m - \frac{L_s L_r}{L_m}) + \frac{L_r}{L_m} \psi_s^{k-1} \tag{13}$$

Therefore, the predictive stator flux is as follows,

$$\psi_s^{k+1} = \psi_s^k + V_o^{k+1} T_s - R_s I_o^{k+1} T_s \tag{14}$$

where V_o^{k+1} is derived from (3) and predictive stator current is,

$$I_o^{k+1} = \psi_r^k (V_o^{k+1} + (\tau_r k_r - j k_r \omega^k)) \frac{T_s}{\sigma L_s} + I_o^k (1 - \frac{T_s r_\sigma}{\sigma L_s}) T_s \tag{15}$$

where, $r_\sigma = R_s + R_r k_r^2$, $\tau_r = \frac{L_r}{R_r}$, $k_s = \frac{L_m}{L_s}$, $k_r = \frac{L_m}{L_r}$ and $\sigma = 1 - k_s k_r$.

Therefore predictive torque of induction motor for the next sampling period is as follows,

$$T_e^{k+1} = \frac{3}{2} p (\psi_s^{k+1} \times I_o^{k+1}) \tag{16}$$

Furthermore, a first order differential equation can be applied for the prediction of the input voltages and input currents if reactive power need to be minimized [21, 40].

3.2 Optimization method of weighting factor

Torque ripple of the induction motor can be presented as below:

$$T_r^2 = \frac{1}{T_s} \int_0^{T_s} (D_T + m_1 t)^2 dt \tag{17}$$

where, $D_T = T_e - T_{nom}$, T_r= Torque ripple, T_s= Sampling time, T_s= Torque of induction motor, T_{nom} = Nominal torque of induction motor, m_1= Ascending torque slope. This ascending slope can be calculated as follows (refer to Appendix: **Case 1**)

$$\begin{aligned} m_1 = -(\frac{R_s}{\sigma L_s} + \frac{R_r}{\sigma L_r}) T_e + K[(V_{oq} \psi_{rd} - V_{od} \psi_{rq}) \\ - \omega^k (\psi_{sd} \psi_{rd} + \psi_{sq} \psi_{rq})] \end{aligned} \tag{18}$$

where,

V_{od} = Stator voltage α-axis component
V_{oq} = Stator voltage β-axis component and

$$K = \frac{3}{2} p, \ \sigma = 1 - k_r k_s = 1 - \frac{L_m^2}{L_r L_s}$$

The simplified torque ripples can be represented as follows:

$$T_r^2 = \frac{1}{T_s}\int_0^{T_s}(D_T^2 + m_1^2 t^2 + 2m_1 t D_T)dt \quad (19)$$

The first derivative of torque ripple to the weighting factor has to be set to zero in order to find the weighting factor that minimizes the ripples of torque. In Eq. (19), only m_1 is related to weighting factor because only this parameter is related to (V_{od}, V_{oq}). The selection of them is based on a cost function. As a results, $T_r^2 = T_r^2(m_1)$, $m_1 = m_1(V_o)$, $V_o = V_o(W_{opt})$

Therefore, $$T_r^2 = T_r^2(W_{opt}), \quad (20)$$

Eq. (19) represents the relation between the ascending slope of torque and torque ripple whereas Eq. (18) is with stator voltage and ascending slope of torque. In the Appendix: **Case 2** it has been explained the relation in between weighting factor and the voltage.

To find the optimum weighting factor in the cost function the derivative of the torque ripple must be zero. Therefore,

$$\frac{dT_r^2}{dW_{opt}} = 0 \quad (21)$$

By solving the first derivative of torque ripple in Eq. (21), it gives optimum weighting factor corresponding to minimum torque ripples. (refer to Appendix **Case 3**)

$$G = \frac{3D_T}{2KT_s} + \omega^k(\psi_{sd}\psi_{rd} + \psi_{sq}\psi_{rq}) + \frac{1}{K}\left(\frac{R_s}{\sigma L_s} + \frac{R_r}{\sigma L_r}\right)T_e \quad (22)$$

$$W_{opt} = \frac{\beta_2\psi_{rd} - \beta_1\psi_{rq}}{G + \psi_{rq}(\alpha_1 + V_{od,k-1}) - \psi_{rd}(\alpha_2 + V_{oq,k-1})} \quad (23)$$

All the symbols used in Eq. (23) are explained in Appendix: **Case 3**. The calculated weighting factor from Eq. (23) is utilized to determine the cost functions for each possible switching state for the IMC.

3.3 Cost function determination

The predicted torque with its nominal value and predicted flux correspond to its reference can be combined in a single term to express the cost function. This is the conventional weighting factor based cost function used in the predictive control algorithm investigated in [23] and [40].

$$g^{k+1} = X_1\left|(T_e^{k+1} - T_{\text{nom}})\right| + X_2\left|(\psi_s^{k+1} - \psi_{ref})\right| \quad (24)$$

In Eq. (24), X_1 and X_2 are the conventional weighting factors and (24) can be used to control the torque and flux for the conventional weighting factor based model predictive control scheme.

On the other hand, the following cost function can be used in the case of weighting factor optimization based predictive control algorithm which has been investigated in [32]:

$$g_w^{k+1} = \frac{1}{2}\left(\left|T_e^{k+1} - T_{nom}\right|^2 + W_{opt}\left|\left|\psi_s^{k+1}\right|^2 - \left|\psi_{ref}\right|^2\right|^2\right) \quad (25)$$

W_{opt}, is the optimized weighting factor. The switching state which produces minimum cost function is selected in the next sampling period T_s to actuate the IMC for the both cases of verifications.

4. Simulation Results and Discussion

The proposed optimum weighting factor based predictive control of induction motor fed by an IMC is verified in MATLAB Simulink environment to justify the performance of the system. In order to compare the torque ripple behaviour with the proposed weighting factor optimization in predictive control scheme corresponding to the conventional weighting factor based predictive control algorithm, both the methods have been investigated separately. In addition, the behavior (torque and flux) of the induction motor are analyzed for rated speed and low speed regions with encouraging performances in the proposed optimum weighting factor based predictive control platform. The parameters used in simulations are given in **Table 1** (refer to Appendix) and the simulations has been carried out with the sampling time, T_s=20 μs.

4.1 Analysis of the results at rated speed region

To investigate torque ripple behavior of induction motor for rated speed region, two cases are analyzed here. First, the validation of the predictive control algorithm is performed with conventional weighting factor, while in the second case, an optimization method is adopted to select the optimized weighting factor for the predictive control algorithm. In both cases, the induction motor starts at 0.01s without any load torque, varying the reference speed from 0 to 149.75 rad/s and the torque is limited to 51 Nm. A load torque of 40 Nm is applied at time of 0.25s and a reverse torque at 0.35s is applied to change the speed in the reverse direction from 149.75 rad/s to -149.75 rad/s. In this investigation, stator reference flux has been assumed as 1.1 Wb in all the verifications.

The speed controller generates torque references at transients which is different from zero and be appreciated as a good tracker of speed given in Figs. 4(a) and 5(a), of torque indicated in Figs. 4(b) and 5(b), of stator flux depicted in Figs. 4(c) and 5(c) in both the conventional and proposed optimum weigthing factor based predictive control schemes, respectively. Also, the stator flux α-β

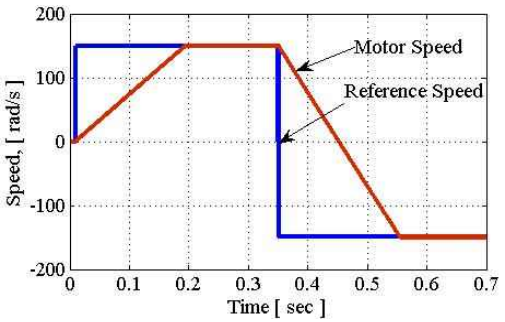

(a)

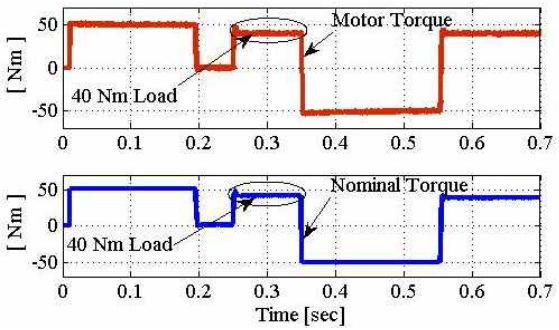

(b)

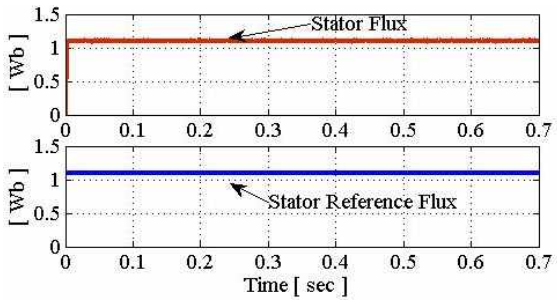

(c)

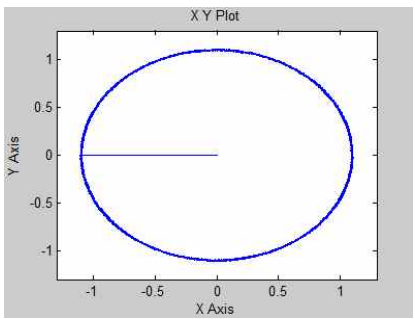

(d)

Fig. 4. Verification results at the rated speed (conventional weighting factor): (a) Motor speed, (ω) [rad/s] and reference speed, (ω_{ref}) [rad/s]; (b) Induction motor torque, (T_e) [Nm] and nominal torque, (T_{nom}) [Nm] (c) Stator flux, (ψ_s) [Wb] and stator reference flux, (ψ_{ref}) [Wb]; (d) α-β presentation for the stator flux, (ψ_s) [Wb].

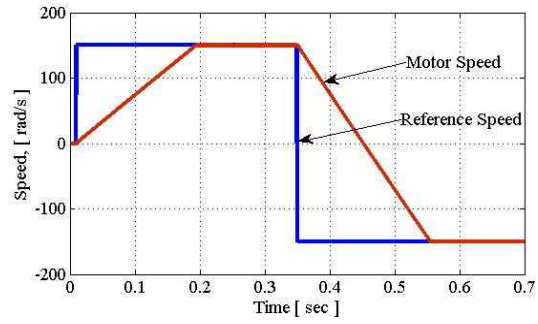

(a)

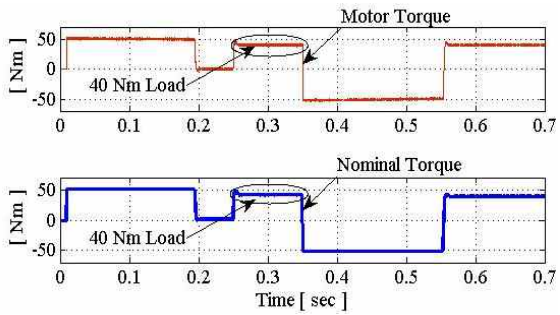

(b)

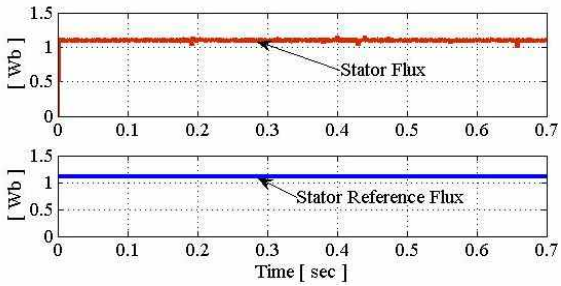

(c)

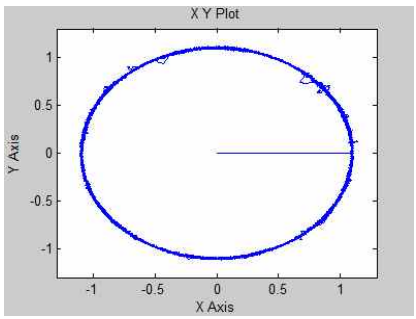

(d)

Fig. 5. Verification results at the rated speed(optimized weighting factor): (a) Motor speed, (ω) [rad/s] and reference speed, (ω_{ref}) [rad/s]; (b) Induction motor torque, (T_e) [Nm] and nominal torque, (T_{nom}) [Nm] (c) Stator flux, (ψ_s) [Wb] and stator reference flux, (ψ_{ref}) [Wb]; (d) α-β plot for stator flux, (ψ_s) [Wb].

representations are plotted in Figs. 4(d) and 5(d) for both cases, respectively and the mentioned figures regarding the stator flux follows the reference magnitude of

around 1.1 Wb, accurately. Furthermore, at time of 0.35s, in Figs. 4(a) and 5(a), the nominal speeds are changed to reverse direction and induction motor follows the reverse nominal speeds starting at 0.35s with reverse maximum torques in Figs. 4(b) and 5(b). At time of 5.5s induction motor attained full reverse rated speed and goes to the regeneration mode.

Case 1: Torque ripples reduction in forward rated speed

The torque ripples for both the conventional weighting factor and proposed optimization of weighting factor are shown in Figs. 6(a) and 6(b), respectively in the forward rated speed of the induction motor to clarify the ripples behavior. For a certain time range of verification in the Fig. 6(a), the maximum value of the torque ripples is 52.40 Nm and the minimum is 47.60 Nm. Therefore the torque ripples is found as 9.41% for the method with conventional weighting factor. The difference between the maximum and minimum torque is 4.8 Nm. On the other hand, for the proposed weighting factor optimization method, the maximum and the minimum values of the torque ripples are in between 51.70 Nm and 49.00 Nm, respectively, in the same time ranges. Consequently, the torque ripples reduces to 5.29% for the proposed weighting factor optimization scheme and the difference between the maximum and minimum value is 2.7 Nm. Therefore, the proposed weighting factor optimization method has improved the results by (9.41%-5.29%) 4.12% torque ripples of the induction motor for the forward rated speed corresponding to conventional weighting factor based predictive control.

Case 2: Torque ripples reduction in reverse rated speed

On the other side, the Figs. 7(a), and 7(b) shows the torque ripples behavior for both cases in reverse rated speed region of the induction motor. In Fig. 7(a), the maximum value of the torque ripple is 41.46 Nm and the minimum value is 38.4 Nm. Therefore the torque ripple variation is 7.94% in the reverse rated speed region of the induction motor with the conventional weighting factor and the difference of the maximum and minimum peak of the torque is 3.06 Nm. Furthermore, the Fig 7(b) shows the torque ripples associated with the optimized weighting factor based predictive control algorithm. In this case, the maximum magnitude of the torque ripple is 40.5 Nm and the minimum torque ripple is 39 Nm. As a result, variation of torque ripples is found as 3.89% for the proposed weighting factor optimization scheme and the difference of peak values is 1.5 Nm. Therefore, the proposed weighting factor optimization method has improved the results by (7.94%-3.89%) 4.05% torque ripples of the induction motor for the reverse rated speed region compared to conventional weighting factor based predictive control algorithm.

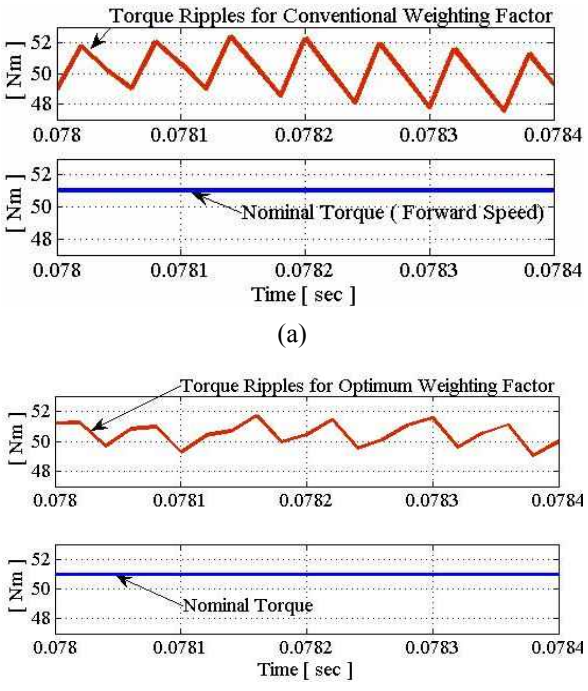

Fig. 6. Torque ripple reduction (forward rated speed): (a) using conventional weighting factor; (b) with imposed weighting factor optimization.

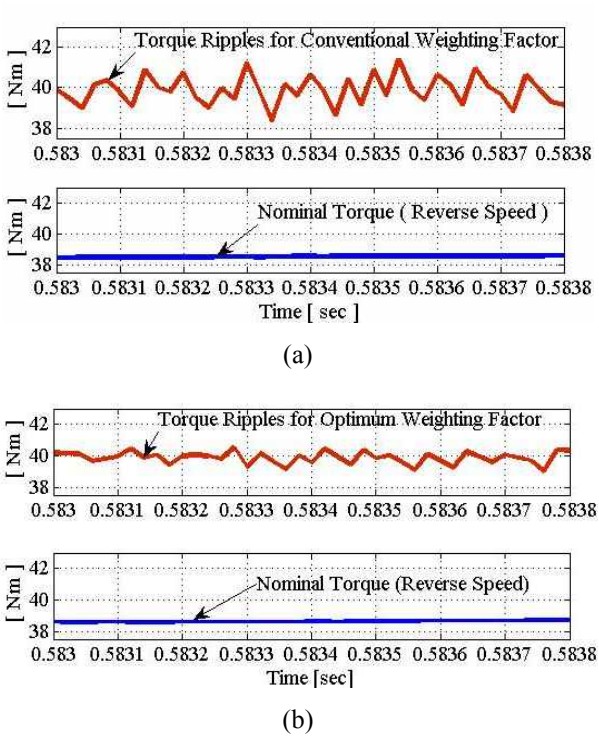

Fig. 7. Torque ripple reduction (reverse rated speed): (a) using conventional weighting factor; (b) with imposed weighting factor optimization.

4.2 Analysis of the results at low speed region

In this study, the induction motor also starts at 0.01s without any load torque, varying the reference speed from 0 to 35 rad/s and the torque is limited to 7 Nm. A load torque of 3 Nm is applied at time of 0.4s and a reverse torque at 0.5s is applied to change the speed in the reverse direction from 35 rad/s to -35 rad/s. In these cases, stator reference flux also assumed as 1.1 Wb. The speed controller also generates torque references at transients which is different from zero and be appreciated as a good tracker of speed given in Figs. 8(a) and 9(a), of torque indicated in Figs. 8(b) and 9(b), of stator flux depicted in Figs. 8(c) and 9(c) in both the conventional and proposed optimum weigthing factor based predictive control schemes, respectively. At time of 0.5s, in Figs. 8(a) and 9(a), the nominal speeds are changed to reverse direction and induction motor follows the fixed reverse nominal low speeds starting at 0.5s with reverse maximum low torques in Figs. 8(b) and 9(b). At time of 0.93s, induction motor attain the setted maximum low reverse speed.

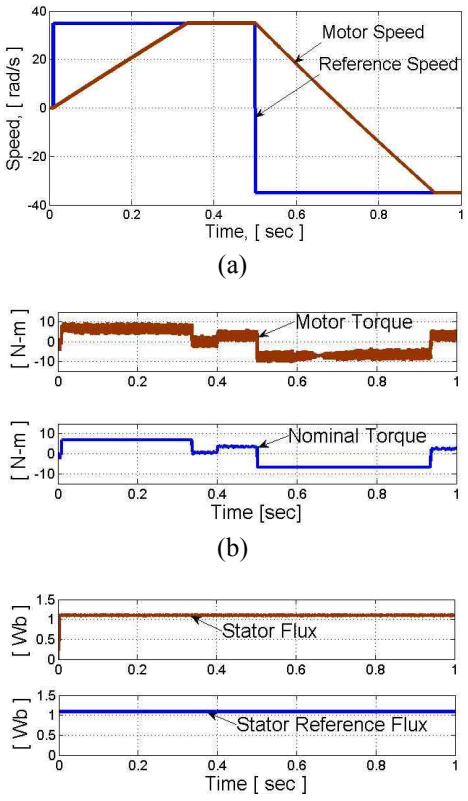

Fig. 8. Verification results (conventional weighting factor): (a) Motor speed, (ω) [rad/s] and reference speed, (ω_{ref}) [rad/s]; (b) Predictive torque, (T_e) [Nm] and Nominal torque, (T_{nom}) [Nm] (c) Stator predictive flux, (ψ_s) [Wb] and stator reference flux, (ψ_{ref}) [Wb].

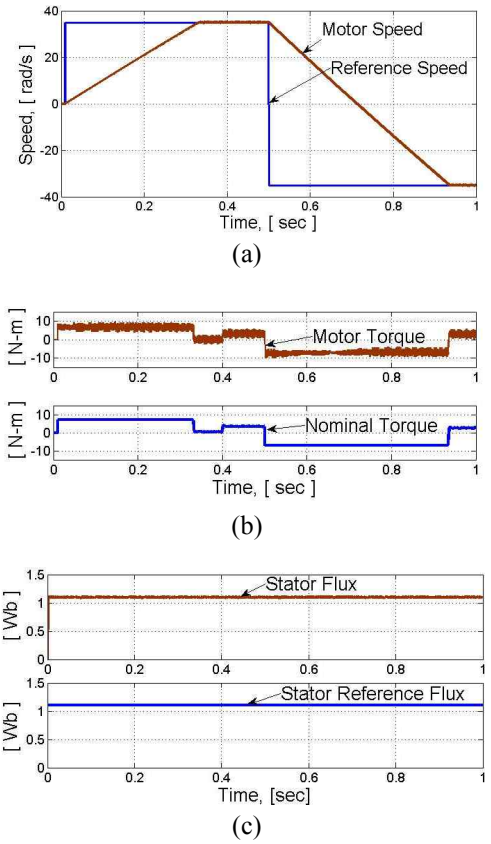

Fig. 9. Verification results (optimized weighting factor): (a) Motor speed, (ω) [rad/s] and reference speed, (ω_{ref}) [rad/s]; (b) Predictive torque, (T_e) [Nm] and Nominal torque, (T_{nom}) [Nm] (c) Stator predictive flux, (ψ_s) [Wb] and stator reference flux, (ψ_{ref}) [Wb].

Case 1: Torque ripples reduction in forward low speed region

In this section, the analysis of torque ripple behavior has been carried out for both the conventional weighting factor and proposed optimization of weighting factor based predictive scheme which are focused in Figs. 10(a) and 10(b), respectively in forward low speed region of the induction motor to justify the ripples behavior. The Fig. 10(a) shows the maximum value of the torque ripple is 5 Nm and the minimum is 1.85 Nm in a certain time range of verification. Therefore, the difference between the maximum and the minimum peak value of the torque ripples is 3.15 Nm for the method of conventional weighting factor. On the other side, for the proposed weighting factor optimization method, the maximum and the minimum acmes of the torque ripples are in between 4 Nm and 2 Nm, respectively in the same time interval and the difference of the values is 2.0 Nm only. Therefore, the proposed weighting factor optimization method has improved the results by (3.15 - 2.0) Nm or 1.15 Nm torque ripples of the induction motor for the forward low speed

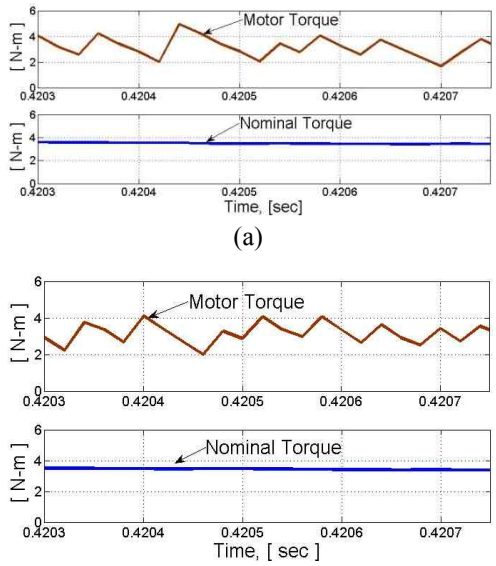

Fig. 10. Torque ripples analysis (forward low speed): (a) using conventional selected weighting factor; (b) with imposed weighting factor optimization.

corresponding to conventional predictive control algorithm.

Case 2: Torque ripples reduction in reverse low speed region

The Fig. 11(a) implies that, the maximum value of the torque ripple is 5.5 Nm and the minimum is 1.1 Nm in a certain time range of verification. Therefore the difference between the maximum and minimum value of the torque ripples is 4.4 Nm for the method of conventional weighting factor. On the other hand, for the proposed weighting factor optimization method, the maximum and the minimum values of the torque ripples are in between 3.6 Nm and 2.2 Nm, respectively. Therefore, the difference of the values is only 1.4 Nm and the proposed weighting factor optimization method has improved the torque ripple by (4.4–1.4) Nm or 3.0 Nm, for the reverse low speed corresponding to conventional weighting factor based predictive control investigation.

In this verification, the input side current of indirect matrix converter is sinosoidal which is shown in Fig. 12. The Fig. 12 shows the relation between the supply voltage and input current to the converter. From the result, it is clear that, in Fig. 12(a), a chaoitic behavior is observed at input current of IMC due to the filter resonance caused by substantial distortion which is created with the harmonic pollution from the supply. As a results, a significant amount of reactive power is generated in the system which can be minimized by adding a reactive power compensation term as the investigation of [23] and the result is shown in Fig. 12(b). Consequently, at the input side of IMC, the current becomes more sinusoidal as well as unity power factor can be achieved.

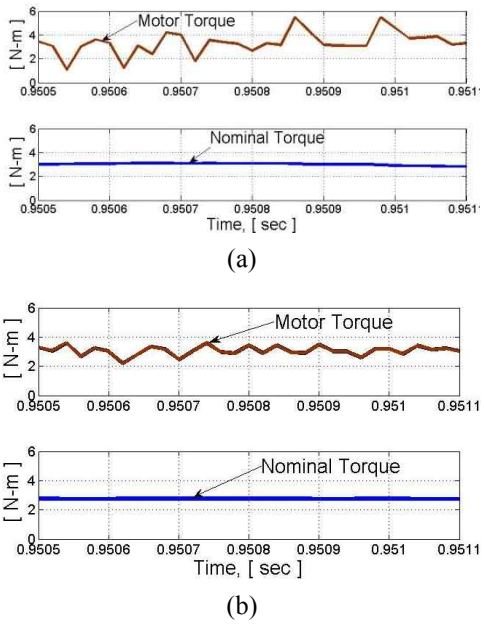

Fig. 11. Torque ripple reduction (reverse low speed): (a) Torque ripples using conventional weighting factor; (b) Torque ripples with imposed weighting factor optimization.

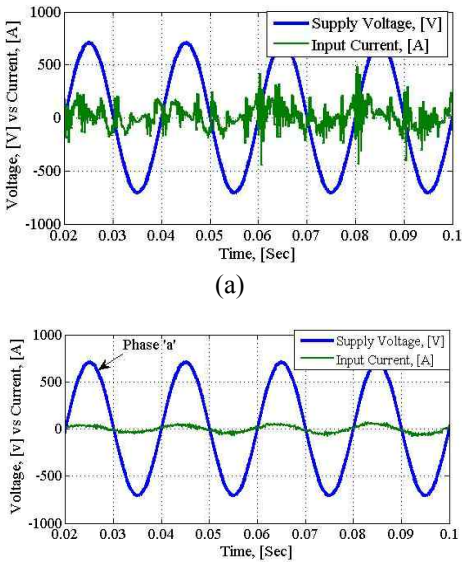

Fig. 12. Supply voltage, V_s^a [V] vs input current, I_i^a [A]: (a) input current of indirect matrix converter with resonance effect; (b) reactive power minimization.

5. Experimental Results and Discussion

An experimental setup design has been carried out to validate the proposed method with experimentation. The experiment has been implemented in DS1104 R&D controller platform with a sampling time of 20 μs for the predictive control algorithm. The experimental setup is

presented in Fig. 13. The parameter of the induction motor are given in Table 2 (refer to Appendix).

The IMC gate signals are generated from the DS1104 R&D controller board. This has been done with compiling the control part of the simulation in the DS1104 R&D controller platform. The predictive three phase load currents, voltages and motor speed was measured with the current sensors, voltage sensors and speed sensors, respectively which were feed backed to the ADC port of the DS1104 R&D controller platform to complete the closed loop of the predictive control algorithm. The Fig. 14 present the results for conventional weighting factor based predictive control method whereas the Fig. 15 is associated with the optimum weighting factor based predictive control of induction motor. The experimental results in Fig. 14 shows the motor starts at 2.6 s and follows the reference speed of 100 rad/s by developing the nominal torque of 5 Nm and the corresponding predictive torque follows the nominal value and it is also 5 Nm. Once obtained the reference speed, the motor predictive torque become minimum value as of nominal torque developed.

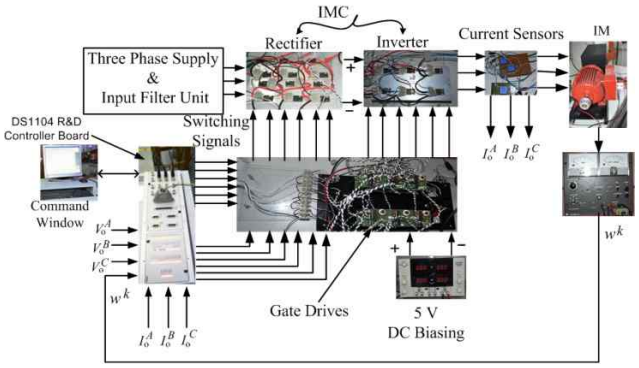

Fig. 13. Experimental setup design.

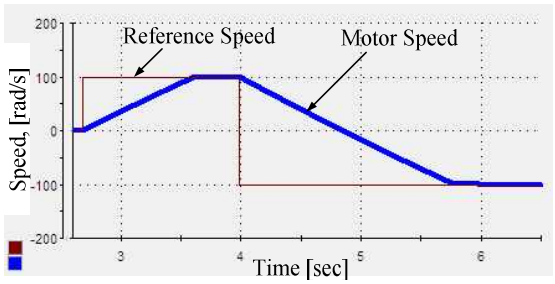

(a)

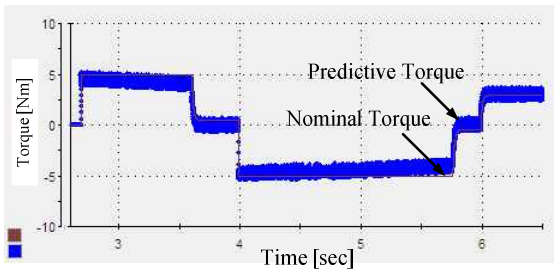

(b)

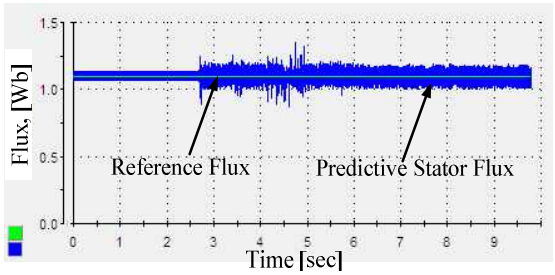

(c)

Fig. 14. Experimental results (conventional weighting factor): (a) Motor speed, (ω) [rad/s] and reference speed, (ω_{ref}) [rad/s]; (b) Predictive torque, (T_e) [Nm] and Nominal torque, (T_{nom}) [Nm] (c) Stator flux, (ψ_s) [Wb] and stator reference flux, (ψ_{ref}) [Wb].

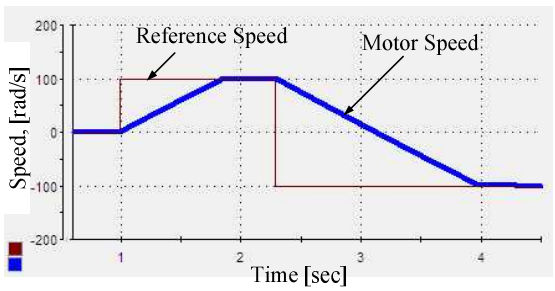

(a)

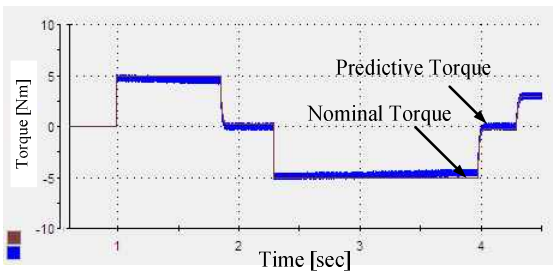

(b)

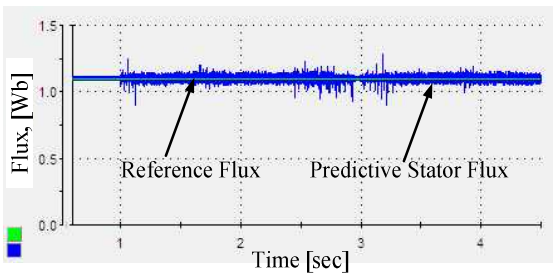

(c)

Fig. 15. Experimental results (optimum weighting factor): (a) Motor speed, (ω) [rad/s] and reference speed, (ω_{ref}) [rad/s]; (b) Predictive torque, (T_e) [Nm] and Nominal torque, (T_{nom}) [Nm] (c) Stator flux, (ψ_s) [Wb] and stator reference flux, (ψ_{ref}) [Wb].

At time 4s, the reference speed changes to reverse direction which developed the reverse 5 Nm nominal torque, and predictive torque follow the reference value. At time 5.5 s, the motor has attained the reverse reference speed and predictive torque also become minimum corresponding to nominal torque. At time of 6 s, it has been applied a load of 3 Nm and the motor predictive torque follows the load torque of 3 Nm. The stator reference flux is taken as 1.1 Wb in this experimentation and the predictive flux also accurately follow the reference value of 1.1 Wb which is presented in Fig. 14 (c). On the other hand, for optimum weighting factor based predictive results follow the similar behavior as changing the time corresponding to conventional results. The only difference between the two methods is in the torque ripple behavior which has been described in Fig. 16.

The Fig. 16(a) presents the conventional torque ripples behavior. The maximum value of the torque ripple is 3.7 Nm and the minimum is 2.35 Nm. The percentage of the torque ripple becomes 46.6% for the conventional weighting factor based predictive control method. In second case, the torque ripple behavior is presented at the Fig. 16(b). In this case, the maximum torque ripple is 3.3 Nm and the minimum value is 2.65 Nm. Therefore, the torque ripple appears 22.4% for the optimum weighting factor based predictive control method. Consequently, the improvement of the torque ripple is 24.2% with the proposed method of optimizing the weighting factor corresponding to conventional one. Therefore, the method is validated with effective reduction of torque ripples. It is noted that, in this paper, the percentage variations are in different level in the simulation and experimentation because of different nominal torque has been considered in both of simulation and experimentation. But in all the cases, it has been achieved a considerable reduction of torque ripple with proposed weighting factor optimization method corresponding to conventional weighting factor based predictive control algorithm.

Finally, the proposed weighting factor optimization method can be applied to minimize the torque ripple in different rated induction motor load with encouraging results.

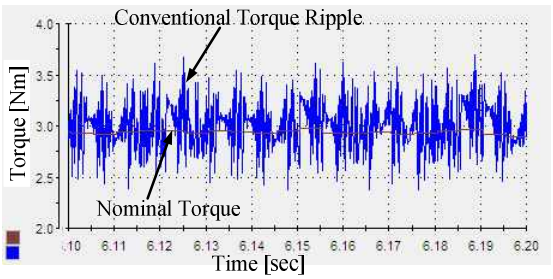

(a)

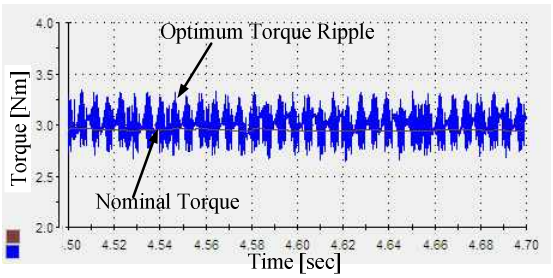

(b)

Fig. 16. Experimental torque ripple reduction: (a) Torque ripples [N-m] using conventional weighting factor; (b) Improved torque ripples [N-m] with imposed weighting factor optimization.

6. Conclusion

Predictive control algorithm with conventional weighting factor and proposed weighting factor optimization methods are presented in this paper in order to reduce the torque ripples and flux control of the induction motor fed by an indirect matrix converter. The proposed method is validated with the MATLAB Simulation and experimentation in the DS1104 R&D controller platform. In this paper, torque ripple reduction behaviors are analyzed for both the rated speed and low speed regions with successful validation of the proposed method. The control scheme has utilized the discrete features of input filter, power converter and inductive load to predict the future behavior of the torque and flux of the system. It has also been employed to obtain the cost functions for 24 possible switching states from which the switching state is selected corresponding to minimum cost function for the next sampling time interval. The system behavior is highly changeable with the values of the weighting factor in the cost function. So, this paper is highlighted with an imposed optimized weighting factor based predictive control to reduce the torque ripples of induction motor and control the flux fed by an IMC corresponding to the conventional predictive control scheme. Finally, predictive control plays a powerful and robust control of torque and flux in both the investigations of the induction motor and the proposed optimization method significantly improve the torque ripple of induction motor in the simulation and experimentation.

Appendix

Case 1: Ascending slope of the torque

The torque for the induction machine can also be determined by the following relation,

$$T_e = T = K(\psi_{sq}\psi_{rd} - \psi_{sd}\psi_{rq}) \tag{26}$$

First derivative of (26) implies the slope of the torque as follows,

$$\frac{dT}{dt}=K(\frac{d}{dt}\psi_{sq}*\psi_{rd}+\frac{d}{dt}\psi_{rd}*\psi_{sq}-\frac{d}{dt}\psi_{sd}*\psi_{rq}-\frac{d}{dt}\psi_{rq}*\psi_{sd}) \tag{27}$$

Considering the induction motor dynamic model from Eq. (27),

$$\frac{dT}{dt}=K[(V_{sq}+W_2)*\psi_{rd}+W_3*\psi_{sq}-(V_{sd}+W_1)*\psi_{rq}-W_4*\psi_{sd}] \tag{28a}$$

$$\begin{bmatrix}W_1\\W_2\\W_3\\W_4\end{bmatrix}=\begin{bmatrix}Q_{11}&Q_{12}&Q_{13}&Q_{14}\\Q_{21}&Q_{22}&Q_{23}&Q_{24}\\Q_{31}&Q_{32}&Q_{33}&Q_{34}\\Q_{41}&Q_{42}&Q_{43}&Q_{44}\end{bmatrix}.\begin{bmatrix}\psi_{sd}\\\psi_{sq}\\\psi_{rd}\\\psi_{rq}\end{bmatrix} \tag{28b}$$

Where,

$$Q_{11}=Q_{22}=-\frac{R_s}{\sigma L_s},\ Q_{13}=Q_{24}=\frac{R_s(1-\sigma)}{\sigma L_m},$$

$$Q_{31}=Q_{42}=\frac{R_r(1-\sigma)}{\sigma L_m},\ Q_{34}=-Q_{43}=\omega^k,$$

$$Q_{33}=Q_{44}=-\frac{R_r}{\sigma L_r},\ Q_{21}=Q_{12}=Q_{32}=Q_{41}=Q_{14}=Q_{23}=0$$

Therefore,

$$\begin{aligned}W_1&=Q_{11}\psi_{sd}+Q_{13}\psi_{rd}\\W_2&=Q_{22}\psi_{sq}+\psi_{24}\psi_{rq}\\W_3&=Q_{31}\psi_{sd}+Q_{33}\psi_{rd}+Q_{34}\psi_{rq}\\W_4&=Q_{42}\psi_{sq}+Q_{43}\psi_{rd}+Q_{44}\psi_{rq}\end{aligned} \tag{29}$$

So, the ascending slope of the torque can be depicted with the following equation,

$$\frac{dT}{dt}=K[(V_{sq}\psi_{rd}-V_{sd}\psi_{rq})+\omega^k(\psi_{sd}\psi_{rd}+\psi_{sq}\psi_{rq})]$$
$$-(\frac{R_s}{\sigma L_s}+\frac{R_r}{\sigma L_r})T_e=m_1 \tag{30}$$

Where, $K=\frac{3}{2}p,\quad \sigma=1-k_rk_s=1-\frac{L_m^2}{L_rL_s}$

Case 2: Weighting factor and voltage relationship

Applying the Taylor expansion around the nominal values in Eq. (25) to express the model predictive variables in a linear manner as follows:

$$T_e=T_{nom}+K(\psi_{rd}^o\Delta\psi_{sq}+\psi_{sq}^o\Delta\psi_{rd}-\psi_{sd}^o\Delta\psi_{rq}-\psi_{rq}^o\Delta\psi_{sd}) \tag{31}$$

$$|\psi_s|^2=|\psi_{ref}|^2+2\psi_{sd}^o\Delta\psi_{sd}+2\psi_{sq}^o\Delta\psi_{sq} \tag{32}$$

Hence, (25) becomes,

$$g^{k+1}=\frac{1}{2}[(\Delta T)^2+W_{opt}(\Delta|\psi_s|^2)^2] \tag{33}$$

Torque and flux displacements are related to stator and rotor flux as follows:

$$Y(t_k)=G.X(t_n) \tag{34a}$$

$$Y=\begin{bmatrix}\Delta T_e\\\Delta|\psi_s|^2\end{bmatrix},\ G=\begin{bmatrix}-K\psi_{rq}^o&K\psi_{rd}^o&K\psi_{sq}^o&-K\psi_{sd}^o\\2\psi_{sd}^o&2\psi_{sq}^o&0&0\end{bmatrix}$$

and

$$X=\begin{bmatrix}\Delta\psi_{sd}\\\Delta\psi_{sq}\\\Delta\psi_{rd}\\\Delta\psi_{sq}\end{bmatrix} \tag{34b}$$

On the other case, in stationary reference frame induction motor discrete model can be described as below:

$$X(t_{k+1})=R.X(t_k)+S.U(t_k) \tag{35a}$$

$$X=\begin{bmatrix}\Delta\psi_{sd}\\\Delta\psi_{sq}\\\Delta\psi_{rd}\\\Delta\psi_{sq}\end{bmatrix},\ U=\begin{bmatrix}\Delta V_{od}\\\Delta V_{oq}\end{bmatrix},\ S=\begin{bmatrix}1&0\\0&1\\0&0\\0&0\end{bmatrix} \tag{35b}$$

$$R=T_s.\begin{bmatrix}\frac{1}{T_s}+Q_{11}&Q_{12}&Q_{13}&Q_{14}\\Q_{21}&\frac{1}{T_s}+Q_{22}&Q_{23}&Q_{24}\\Q_{31}&Q_{32}&\frac{1}{T_s}+Q_{33}&Q_{34}\\Q_{41}&Q_{42}&Q_{43}&\frac{1}{T_s}+Q_{44}\end{bmatrix} \tag{35c}$$

The parameters regarding the matrix R have been introduced before in (28b). For discrete nature of the system considering in the next sampling periods the before mentioned equations gives:

$$Y(t_{k+1})=G.X(t_{k+1})=G.R.X(t_k)+G.S.U(t_k) \tag{36}$$

The appropriate input vector satisfies the following set of equations

$$\begin{aligned}\frac{\delta}{\delta\Delta V_{od}}g_w=0\\\frac{\delta}{\delta\Delta V_{oq}}g_w=0\end{aligned} \tag{37}$$

From Eqs. (25), (36) and (37) lead to the following voltage displacement

$$\Delta V_{od}=\alpha_1+\frac{\beta_1}{W_{opt}} \tag{38a}$$

$$\Delta V_{oq} = \alpha_2 + \frac{\beta_2}{W_{opt}} \tag{38b}$$

Where,

$$\alpha_1 = \frac{-f_1(e_{22}^2 e_{11} - e_{12}e_{21}e_{22})}{(e_{11}e_{22} + e_{12}e_{21})^2}, \beta_1 = \frac{-f_2(e_{12}^2 e_{21} - e_{11}e_{22}e_{12})}{(e_{11}e_{22} + e_{12}e_{21})^2},$$
$$\alpha_2 = \frac{-f_1(e_{21}^2 e_{12} - e_{11}e_{21}e_{22})}{(e_{11}e_{22} + e_{12}e_{21})^2}, \beta_2 = \frac{-f_2(e_{11}^2 e_{22} - e_{11}e_{12}e_{21})}{(e_{11}e_{22} + e_{12}e_{21})^2} \tag{39a}$$

$$\begin{bmatrix} f_1 \\ f_2 \end{bmatrix} = G.R. \begin{bmatrix} \Delta\psi_{sd} \\ \Delta\psi_{sq} \\ \Delta\psi_{rd} \\ \Delta\psi_{sq} \end{bmatrix} \tag{39b}$$

$$\begin{bmatrix} e_{11} & e_{12} \\ e_{21} & e_{22} \end{bmatrix} = \begin{bmatrix} -KT_s\psi_{rq}^o & KT_s\psi_{rd}^o \\ 2T_s\psi_{sd}^o & 2T_s\psi_{sq}^o \end{bmatrix} \tag{39c}$$

These equations are expressed the stator voltage and weighting factor relationship.

Case 3: Optimization of weighting factor

Let, derivative of the torque ripples with respect to weighting factor equals to zero

$$\frac{dT_r^2}{dW_{opt}} = \frac{d}{dW_{opt}}(m_1^2 . \frac{T_s^2}{3} + m_1 D_T T_s + D_T^2) = 0 \tag{40}$$

Therefore, $$\frac{dm_1}{dW_{opt}} = 0 \tag{41}$$

And, $$(m_1 . \frac{2}{3} T_s^2 + D_T T_s) = 0 \tag{42a}$$

$$m_1 = -\frac{3D_T}{2T_s} \tag{42b}$$

From Eqs. (18) and (41) the relation obtained as below;

$$\frac{dm_1}{dW_{opt}} = \frac{d}{dW_{opt}}[K\{(V_{oq}\psi_{rd} - V_{od}\psi_{rq}) + \omega^k(\psi_{sd}\psi_{rd} + \psi_{sq}\psi_{rq})\}$$
$$-(\frac{R_s}{\sigma L_s} + \frac{R_r}{\sigma L_r})T_e] \tag{43a}$$

It gives, $$\psi_{rd}\frac{d}{dW_{opt}}V_{oq} = \psi_{rq}\frac{d}{dW_{opt}}V_{od} \tag{43b}$$

The derivatives of the stator voltage to the weighting factor are obtained as:

$$\frac{d}{dW_{opt}}V_{od} = \frac{d}{dW_{opt}}(V_{od}^o + \Delta V_{od})$$
$$= \frac{d}{dW_{opt}}(\Delta V_{od}) = -\frac{\beta_1}{W_{opt}^2} \tag{44a}$$

$$\frac{d}{dW_{opt}}V_{oq} = \frac{d}{dW_{opt}}(V_{oq}^o + \Delta V_{oq})$$
$$= \frac{d}{dW_{opt}}(\Delta V_{oq}) = -\frac{\beta_2}{W_{opt}^2} \tag{44b}$$

As a result, Eq. (41) is not a suitable equation to calculate the optimized weighting factor parameter because of each cancel from both sides of the Eq. (43).

So, Eqs. (42a) and (42b) is the best criterion for weighting factor optimization.

Therefore,

$$-\frac{3D_T}{2T_s} = K[(V_{oq}\psi_{rd} - V_{od}\psi_{rq}) - \omega^k(\psi_{sd}\psi_{rd} + \psi_{sq}\psi_{rq})]$$
$$-(\frac{R_s}{\sigma L_s} + \frac{R_r}{\sigma L_r})T_e \tag{45}$$

where, $$G = V_{oq}\psi_{rd} - V_{od}\psi_{rq} \tag{46}$$

The Eq. (46) is the criterion for weighting factor

Table 1. Simulation parameters (rated speed and low speed of induction motor)

Description	Variables	Values
Sampling time	T_s	20 μs
Supply phase voltage (RMS)	V_s	500 V
Supply frequency	f_s	50 Hz
Input filter resistance	R_f	0.5 Ω
Input filter inductance	L_f	400 μH
Input filter capacitance	C_f	21 μF
Reference rated speed and low speed	ω_{ref}	149.75 rad/s and 35 rad/s
Nominal torque for rated and low speed	T_{nom}	51 Nm and 7 Nm respectively
Stator resistance	R_s	1.35 Ω
Stator inductance	L_s	0.2861 mH
Rotor resistance	R_r	7.2037 Ω
Rotor inductance	L_r	0.2861 mH
Mutual inductance	L_m	0.2822 mH
Number of poles	P	2
Weighting factor	X_1	63
Weighting factor	X_2	13500

Table 2. Induction motor parameter in the experimentation

Description	Variables	Values
Reference speed	ω_{ref}	100 rad/s
Nominal torque	T_{nom}	5 Nm
Reference flux	ψ_{ref}	1.1 Wb
Stator resistance	R_s	21 Ω
Stator inductance	L_s	1.053 mH
Rotor resistance	R_r	22.63 Ω
Rotor inductance	L_r	1.081 mH
Mutual inductance	L_m	0.9963 mH
Number of poles	p	2
Moment of inertia	J	0.04 Kg m^2

optimization. Combining the Eqs. (38) and (46) optimized weighting factor will be obtained successfully.

Acknowledgements

The authors wish to thank the financial support from the University of Malaya through HIR-MOHE project UM.C/HIR/MOHE/ENG/17 and UMRG project No. RP006E-13 ICT.

References

[1] G. S. Buja and M. P. Kazmierkowski, "Direct torque control of PWM inverter-fed AC motors-a survey," *IEEE Transactions Industrial Electronics,* vol. 51, pp. 744-757, 2004.

[2] M. Rivera, "Predictive control in an Indirect Matrix converter," *Universidad Técnica Federico Santa María,* Valparaiso, Chile, 2011.

[3] J. Beerten, J. Verveckken, and J. Driesen, "Predictive direct torque control for flux and torque ripple reduction," *IEEE Transactions on Industrial Electronics,* vol. 57, pp. 404-412, 2010.

[4] P. W. Wheeler, J. Rodriguez, J. C. Clare, L. Empringham, and A. Weinstein, "Matrix converters: a technology review," *IEEE Trans. Ind. Elec.,* vol. 49, pp. 276-288, 2002.

[5] J. W. Kolar, F. Schafmeister, S. D. Round, and H. Ertl, "Novel three-phase AC-AC sparse matrix converters," *IEEE Transactions on Power Electronics,* vol. 22, pp. 1649-1661, 2007.

[6] P. W. Wheeler, J. C. Clare, L. Empringharn, M. Bland, and M. Apap, "Gate drive level intelligence and current sensing for matrix converter current commutation," *IEEE Transactions on Industrial Electronics,* vol. 49, pp. 382-389, 2002.

[7] K.-B. Lee and F. Blaabjerg, "Sensorless DTC-SVM for induction motor driven by a matrix converter using a parameter estimation strategy," *IEEE Trans. Ind. Elec.,* vol. 55, pp. 512-521, 2008.

[8] S. Mekhilef and M. A. Kadir, "Novel vector control method for three-stage hybrid cascaded multilevel inverter," *IEEE Transactions on Industrial Electronics,* vol. 58, pp. 1339-1349, 2011.

[9] S. Mekhilef and A. Kadir, "Voltage control of three-stage hybrid multilevel inverter using vector transformation," *IEEE Trans. Power Elec.,* vol. 25, pp. 2599-2606, 2010.

[10] K. Menshawi, M. Abdulkader, and S. Mekhilef, "Voltage vector approximation control of multistage-multilevel inverter using simplified logic implementation," in *Proc. IEEE Ninth International Conf. on Power Elec. and Drive Systems (PEDS)*, 2011, pp. 57-65.

[11] S. Mekhilef, M. AbdulKadir, and Z. Salam, "Digital Control of Three Phase Three-Stage Hybrid Multilevel Inverter," *IEEE Transactions on Industrial Informatics,* vol. 9, pp. 719-727, 2013.

[12] A. Ajami, M. R. J. Oskuee, A. Mokhberdoran, and M. T. Khosroshahi, "Advanced Cascade Multilevel Converter with Reduction in Number of Components," *Journal of Electrical Engineering & Technology,* vol. 9, pp. 127-135, 2014.

[13] A. M. Omar, N. A. Rahim, and S. Mekhilef, "Three-phase synchronous PWM for flyback converter with power-factor correction using FPGA ASIC design," *IEEE Trans. Ind. Elec.,* vol. 51, pp. 96-106, 2004.

[14] S. Mekhilef, N. Rahim, and A. Omar, "Modelling of three-phase uniform symmetrical sampling digital PWM for power converter," in *Proc. IEEE 35th Annual Power Electronics Specialists Conf.*, 2004, pp. 3499-3503.

[15] S. Muslem Uddin, P. Akter, S. Mekhilef, M. Mubin, M. Rivera, and J. Rodriguez, "Model predictive control of an active front end rectifier with unity displacement factor," in *Proc. IEEE International Conference on Circuits and Systems (ICCAS)* Kuala Lumpur, Malaysia, 2013, pp. 81-85.

[16] M. Parvez, S. Mekhilef, N. M. Tan, and H. Akagi, "Model predictive control of a bidirectional AC-DC converter for V2G and G2V applications in electric vehicle battery charger," in *IEEE Transportation Electrification Conference and Expo (ITEC)*, 2014, pp. 1-6.

[17] J.Rodriguez, J.Pontt, C.A. Silva, P.Correa, P.Lezana, P. Cortés, and U. Ammann, "Predictive current control of a voltage source inverter," *IEEE Transactions on Industrial Electronics,* vol. 54, pp. 495-503, 2007.

[18] M. Rivera, J. Rodriguez, B. Wu, J. R. Espinoza, and C. A. Rojas, "Current control for an indirect matrix converter with filter resonance mitigation," *IEEE Transactions on Industrial Electronics,* vol. 59, pp. 71-79, 2012.

[19] V. Yaramasu and B. Wu, "Predictive control of three-level boost converter and NPC inverter for high power PMSG-based medium voltage wind energy conversion systems," *IEEE Transactions on Power Electronics,* vol. 29, pp. 5308 - 5322, 2014.

[20] H.-W. Sim, J.-S. Lee, and K.-B. Lee, "On-line Parameter Estimation of Interior Permanent Magnet Synchronous Motor using an Extended Kalman Filter," *Journal of Electrical Engineering & Technology,* vol. 9, pp. 600-608, 2014.

[21] P. Correa, J. Rodríguez, M. Rivera, J. R. Espinoza, and J. W. Kolar, "Predictive control of an indirect matrix converter," *IEEE Transactions on Industrial Electronics,* vol. 56, pp. 1847-1853, 2009.

[22] J. Rodriguez, J. Kolar, J. Espinoza, M. Rivera, and C. Rojas, "Predictive current control with reactive power minimization in an indirect matrix converter," in *Proc. IEEE International Conf. on Ind. Tech.*

(ICIT), 2010, pp. 1839-1844.
[23] S. Muslem Uddin, S. Mekhilef, M. Rivera, and J. Rodriguez, "A FCS-MPC of an induction motor fed by indirect matrix converter with unity power factor control," in *Proc. 8th IEEE Conference on Industrial Electronics and Applications (ICIEA)* Melbourne, Australia, 2013, pp. 1769-1774.
[24] M. Rivera, J. Rodriguez, J. R. Espinoza, T. Friedli, J. W. Kolar, A. Wilson, and C. A. Rojas, "Imposed sinusoidal source and load currents for an indirect matrix converter," *IEEE Transactions on Industrial Electronics,* vol. 59, pp. 3427-3435, 2012.
[25] V. Yaramasu and B. Wu, "A Model Predictive Decoupled Active and Reactive Power Control for High Power Grid-Connected Four-Level Diode-Clamped Inverters," *IEEE Transactions on Industrial Electronics,* vol. 61, pp. 3407-3416, 2014.
[26] J. Rodriguez, J. Pontt, P. Correa, P. Lezana, and P. Cortes, "Predictive power control of an AC/DC/AC converter," in *Proc. Fourtieth IAS Annual Meeting Conference Record of Industry Applications* 2005, pp. 934-939.
[27] P.Cortés and J.Rodríguez, "Three-phase inverter with output LC filter using predictive control for UPS applications," in *Proc. European Conference on Power Electronics and Applications* 2007, pp. 1-7.
[28] P. Cortés, J. Rodríguez, D. E. Quevedo, and C. Silva, "Predictive current control strategy with imposed load current spectrum," *IEEE Transactions on Power Electronics,* vol. 23, pp. 612-618, 2008.
[29] R. Vargas, P. Cortes, U. Ammann, J. Rodríguez, and J. Pontt, "Predictive control of a three-phase neutral-point-clamped inverter," *IEEE Transactions on Industrial Electronics,* vol. 54, pp. 2697-2705, 2007.
[30] R. Vargas, U. Ammann, J. Rodriguez, and J. Pontt, "Predictive strategy to reduce common-mode voltages on power converters," in *Proc. IEEE Power Electronics Specialists Conference*, 2008, pp. 3401-3406.
[31] P. Cortes, S. Kouro, B. La Rocca, R. Vargas, J. Rodriguez, J.I. Leon, S. Vazquez, and L.G. Franquelo, "Guidelines for weighting factors design in model predictive control of power converters and drives," in *Proc. IEEE International Conference on Industrial Technology, ICIT*, Gippsland, VIC, 2009, pp. 1-7.
[32] S. A. Davari, D. A. Khaburi, and R. Kennel, "An Improved FCS – MPC Algorithm for an Induction Motor With an Imposed Optimized Weighting Factor," *IEEE Transactions on Power Electronics,* vol. 27, pp. 1540-1551, 2012.
[33] M. Uddin, S. Mekhilef, M. Rivera, and J. Rodriguez, "Predictive indirect matrix converter fed torque ripple minimization with weighting factor optimization," in *International Power Electronics Conference (IPEC-Hiroshima 2014-ECCE-ASIA)*, 2014, pp. 3574-3581.
[34] M. Uddin, S. Mekhilef, M. Mubin, M. Rivera, and J. Rodriguez, "Model Predictive Torque Ripple Reduction with Weighting Factor Optimization Fed by an Indirect Matrix Converter," *Electric Power Components and Systems,* vol. 42, pp. 1-11, 2014.
[35] S. A. Davari, D. A. Khaburi, and R. Kennel, "Using a weighting factor table for FCS-MPC of induction motors with extended prediction horizon," in *Proc. IEEE 38th Annual Conference on Industrial Electronics Society*, 2012, pp. 2086-2091.
[36] C. Rojas, J. Rodriguez, F. Villarroel, J. Espinoza, C. Silva, and M. Trincado, "Predictive Torque and Flux Control Without Weighting Factors," *IEEE Transactions on Industrial Electronics,* vol. 60, pp. 681-690, 2013.
[37] Z. Boulghasoul, L. El Bahir, A. Elbacha, and E. Elwarraki, "Adaptive-Predictive Controller based on Continuous-Time Poisson-Laguerre Models for Induction Motor Speed Control Improvement," *Journal of Electrical Engineering & Technology,* vol. 9, pp. 908-925, 2014.
[38] P.-W. Han, "The Study of the Stray Load Loss and Mechanical Loss of Three Phase Induction Motor considering Experimental Results," *Journal of Electrical Engineering & Technology,* vol. 9, pp. 121-126, 2014.
[39] J. Rodriguez, J. Kolar, J. Espinoza, M. Rivera, and C. Rojas, "Predictive torque and flux control of an induction machine fed by an indirect matrix converter," in *Proc. IEEE International Conf. on Ind. Tech.*, 2010, pp. 1857-1863.
[40] J. Rodriguez, J. Kolar, J. Espinoza, M. Rivera, and C. Rojas, "Predictive torque and flux control of an induction machine fed by an indirect matrix converter with reactive power minimization," in *Proc. IEEE International Symposium on Industrial Electronics*, 2010, pp. 3177-3183.

Muslem Uddin received the B.Sc. degree in electrical and electronic engineering from the Chittagong University of Engineering and Technology (CUET), Bangladesh, in 2009. Currently he is continuing M.Sc. degree and working as a research assistant with the 'Power Electronics and Renewable Energy Research Laboratory (PEARL)', department of electrical engineering, University of Malaya, Malaysia. He has worked as a research assistant with the department of electrical and electronic engineering, Chittagong University of Engineering and Technology (CUET), Bangladesh, from October'2009 to August'2010. Also, he is working as a Lecturer with the department of electrical and electronic engineering, University of Information Technology and Sciences (UITS), Bangladesh, from September' 2010. His research interests includes power converter control and

drives, predictive and digital control, direct and indirect matrix converters, high voltage engineering and renewable energy.

Saad Mekhilef received the B.Eng. degree in Electrical Engineering from the University of Setif, Setif, Algeria, in 1995, and the Master of Engineering Science and Ph.D. degrees from the University of Malaya, Kuala Lumpur, Malaysia, in 1998 and 2003, respectively. He is currently a Professor at the Department of Electrical Engineering, University of Malaya, Kuala Lumpur. He is the author or coauthor of more than 250 publications in international journals and proceedings. He is a Senior Member of the IEEE. He is actively involved in industrial consultancy, for major corporations in the power electronics projects. His research interests include power conversion techniques, control of power converters, renewable energy and energy efficiency.

Marco Rivera received his B.Sc. in Electronics Engineering and M.Sc. in Electrical Engineering from the Universidad de Concepcion, Chile, in 2007 and 2008, respectively. He received the PhD degree at the Department of Electronics Engineering, Universidad Tecnica Federico Santa Maria, in Valparaiso, Chile, in 2011 with a scholarship from the Chilean Research Fund CONICYT. During 2011 and 2012 he was working on a Post-Doctoral position and as part-time professor of Digital Signal Processors and Industrial Electronics at Universidad Tecnica Federico Santa Maria and currently, he is a professor at Universidad de Talca, Chile. He is a Member of the IEEE. His research interests include matrix converters, predictive and digital controls for high-power drives, four-leg converters, renewable energies and development of high performance control platforms based on Field-Programmable Gate Arrays.

Jose Rodriguez received the Engineering degree in electrical engineering from Universidad Técnica Federico Santa María (UTFSM), Valparaíso, Chile, in 1977 and the Dr.-Ing. Degree in electrical engineering from the University of Erlangen, Erlangen, Germany, in 1985. He has been with the Department of Electronics Engineering, Since 1977, where he is currently full Professor and Rector. He has coauthored more than 350 journal and conference papers. He is a Fellow of the IEEE and is a member of the Chilean Academy of Engineering. His main research interests include multilevel inverters, new converter topologies, control of power converters, and adjustable-speed drives.